doi.org/10.26434/chemrxiv.5327677.v1

How toxicity of nanomaterials towards different species could be simultaneously evaluated: Novel multi-nano-read-across approach

Natalia Sizochenko, Alicja Mikolajczyk, Karolina Jagiello, Tomasz Puzyn, Jerzy Leszczynski, Bakhtiyor Rasulev

Submitted date: 20/08/2017 • Posted date: 31/08/2017

Citation information: Sizochenko, Natalia; Mikolajczyk, Alicja; Jagiello, Karolina; Puzyn, Tomasz; Leszczynski, Jerzy; Rasulev, Bakhtiyor (2017): How toxicity of nanomaterials towards different species could be simultaneously evaluated: Novel multi-nano-read-across approach. ChemRxiv. Preprint.

Application of predictive modeling approaches is able solve the problem of the missing data. There are a lot of studies that investigate the effects of missing values on qualitative or quantitative modeling, but only few publications have been
discussing it in case of applications to nanotechnology related data. Current project aimed at the development of multi-nano-read-across modeling technique that helps in predicting the toxicity of different species: bacteria, algae, protozoa, and mammalian cell lines. In this study, the experimental toxicity for 184 metal- and silica oxides (30 unique chemical types) nanoparticles from 15 experimental datasets was analyzed. A hybrid quantitative multi-nano-read-across approach that combines interspecies correlation analysis and self-organizing map analysis was developed. At the first step, hidden patterns of toxicity among the nanoparticles were identified using a combination of methods. Then the developed model that based on categorization of metal oxide nanoparticles' toxicity outcomes was evaluated by means of combination of supervised and unsupervised machine learning techniques to find underlying factors responsible for toxicity.

File list (2)

How toxicity of nanomaterials towards different species could be simultaneously evaluated: Novel multi-nano-read-across approach

Natalia Sizochenko,[a,b,c] Alicja Mikolajczyk,[a,b] Karolina Jagiello,[a] Tomasz Puzyn,[a] Jerzy Leszczynski[b]† and Bakhtiyor Rasulev[b,c]†

Application of predictive modeling approaches is able solve the problem of the missing data. There are a lot of studies that investigate the effects of missing values on qualitative or quantitative modeling, but only few publications have been discussing it in case of applications to nanotechnology related data. Current project aimed at the development of multi-nano-read-across modeling technique that helps in predicting the toxicity of different species: bacteria, algae, protozoa, and mammalian cell lines. In this study, the experimental toxicity for 184 metal- and silica oxides (30 unique chemical types) nanoparticles from 15 experimental datasets was analyzed. A hybrid quantitative multi-nano-read-across approach that combines interspecies correlation analysis and self-organizing map analysis was developed. At the first step, hidden patterns of toxicity among the nanoparticles were identified using a combination of methods. Then the developed model that based on categorization of metal oxide nanoparticles' toxicity outcomes was evaluated by means of combination of supervised and unsupervised machine learning techniques to find underlying factors responsible for toxicity.

Introduction

Significance of nanotechnology is rapidly increasing along with the development of new nanomaterials.[1] There are several important issues that should be addressed prior to introduction of new nanomaterials to the market. Such issues are related to the comprehension of interactions patterns between nanoparticles and living cells and organisms. This influences toxicity and environmental effects on nanomaterials. Unusual structures, a large diversity of nanomaterials and variations of their physicochemical properties are major obstacles on the way of development of the appropriate guidelines or standards for safety testing of nanomaterials.[2] Studies reported in the literature have delivered limited principles that could be applied to comprehend complex biological action of nanoparticles.[3] Moreover, considering that the process of nanoparticles investigation is complicated, time consuming and limited due to high cost of *in vivo* and *in vitro* tests, it is still difficult to provide a sufficient safety information for each particular type of nanoparticles. In consequence, it means, that available datasets have data gaps that need to be filled in order to perform the comprehensive safety assessment of nanomaterials.

[a.] *Laboratory of Environmental Chemometrics, Institute for Environmental and Human Health Protection, Faculty of Chemistry, University of Gdansk, Gdansk, Poland.*
[b.] *Interdisciplinary Nanotoxicity Center, Department of Chemistry and Biochemistry, Jackson State University, Jackson MS, USA.*
[c.] *Department of Coatings and Polymeric Materials, North Dakota State University, Fargo, ND, USA.*
† corresponding authors: jerzy@icnanotox.org; bakhtiyor.rasulev@ndsu.edu
Electronic Supplementary Information (ESI) available:

The implementation of REACH (Registration, Evaluation, Authorisation and Restriction of Chemicals) legislation policy aims at filling of the gaps in the toxicity data. Various experimental and theoretical tools have been developed to tackle the problem of scarce data. In particular, REACH policy works through the combination of the cheminformatics approaches with experimental testing.[4–7] Such combination leads to the significant minimization of the required number of animal tests.

Within the last ten years, cheminformatics experts developed more than fifty models related to nanoparticles' toxicity (so-called nano-QSAR, QNAR, nano-categorization, and nano-read-across models).[7,8] However, most of these models are applicable only to prediction of one type of organism/cell response, each. Moreover, these predictive models did not address the problem of the missing data in these datasets. Hence, there is a lack of models for nanoparticles that could be applied to fill data gaps for two or more endpoints simultaneously. At the same time, previously, it has been successfully done for organic compounds, so indeed one expects that it also possible to generate global models for nanomaterials.[9]

However, there are still a lot of difficulties to correlate descriptors (for example, theoretical physicochemical properties of nanoparticles) with multiple toxicities. This is because mechanisms of nanoparticle's action could be different for different species and at different external environmental conditions (such as pH, protein corona, etc.).[10]

Based on the above, the careful evaluation of nanoparticles' datasets using data mining techniques is highly needed to overcome uncertainties related to similarity/dissimilarity in

patterns of nanoparticle's action. For this purpose, the categorization tools could be applied. Categorization approaches are techniques that predict endpoint information for one chemical by using data from the same endpoint from another chemical, which is considered to be 'similar' in some way.[11] For instance, the relevant attributes may include cytotoxicity outcomes, environmental endpoints (e.g., aquatic toxicity), physicochemical parameters, etc. Recently, four categories of concepts of grouping, equivalence, read-across and non-classified concept have been introduced.[11]

All mentioned concepts are based on idea of dataset splitting between different groups. The group represents the pool of nanomaterials that share a commonality relevant for risk assessment. It can be one or more common property(ies) in a physical, chemical, exposure, (eco)toxicological, toxicokinetics or environmental fate sense.[12] Results of preliminary categorization of metal oxide nanoparticles (MeOx NPs) could be a useful tool for early detection of hazardous or safe materials as it was demonstrated by *Gajewicz et al.*,[13] *Oomen et al*. ,[12] *Arts et al.*[14] and *Fjodorova et al.*[15]

However, data science also stumbled upon some limitations related to unknown or missing values in available datasets. Incomplete observations can adversely affect the operation of machine learning algorithms. It is important to find if the features of endpoints were missed at induction time ("training set") or at the prediction time ("external validation set" or "test set").[16] To handle this, the exploration of imputation methods is highly recommended. In general, common imputation methods are based on: 1) removing entire observations with missed values; 2) filling in the missed data with the most frequent values; 3) filling in unknown values by correlations; 4) filling in missed values by similarities between cases. In cheminformatics, third and fourth cases are often applied. For instance, the read-across approach is data gap filling technique that is based on external predictions for untested compounds using data of toxicity or any other endpoint. In other words, read-across is able to predict information on one or more endpoints of one nanoparticle or more nanoparticles using data (experimental or calculated) from other nanoparticles.

Currently, cluster analysis and self-organizing maps (SOM) categorization approaches represent useful and proven data science tools for analysis of hidden patterns within multidimensional data.[17,18] SOM analysis provides an ordered two-dimensional visualization of data, where nanoparticles with similar patterns of action are grouped in SOM units.[17]

In our study, multi-task nano-read across approach is developed to analyze and fill gaps in vital fifteen toxicity datasets. A SOM analysis combined with the interspecies correlation was applied for data mining of the nanoparticles' toxicities library. Here, we attempted to compare toxicity mechanisms for malicious and healthy cells, bacteria, algae and protozoa. This study is a logical continuation and significant extension of our previous articles, when the differences between the mechanisms of toxicity of metal oxide nanoparticle for two species: prokaryotic and eukaryotic systems were analyzed.[10,19]

Materials and methods

Datasets

The main text of the article should appear here with headings as appropriate. In this study the *in vitro* cytotoxicity data (denoted as EC_{50}/IC_{50} – the effective concentration of a compound that brings about a 50% reduction in bacteria/cell viability) of various metal oxide nanoparticles were gathered from different sources. We considered fifteen datasets: bacteria *Escherichia coli* (four datasets),[20–22] bacteria *Photobacterium phosphoreum,*[23] bacteria *Vibrio fischeri,*[24] human keratinocyte cell line *HaCaT,*[19,25] epithelial cell line *A549* (two datasets),[26,27] human epithelial colorectal cell line *Caco2* (two datasets),[26,27] murine fibroblast cell line *Balb/c 3T3* (two datasets),[26,27] microalga *Pseudokirchneriella subcapitata,*[24] and protozoan *Tetrahymena thermophile*.[24]

In the case of *E. coli*, dataset №1, the duration of exposure was two hours in dark conditions[20] and in the case of *E. coli,* datasets №2 and №3, the duration of exposure was thirty minutes under dark conditions and under light conditions, respectively.[21] In the case of *E. coli*, dataset №4, the duration of exposure was 24h under dark conditions.[22] For *A549* cells, *Caco2* cells and *Balb/c 3T3* cells we gathered two datasets. For datasets denotes as № 1 the exposure time was 12 hours, for datasets with mark № 2 the exposure time was 24 hours.[26,27]

Initial data was grouped and standardized. The IC_{50} and EC_{50} values were converted to the same molar scale [mol/L]. The inverse data of the IC_{50} and EC_{50} were transformed to the logarithmic scale (negative-transformed): log $1/EC_{50}$ and log $1/IC_{50}$. Collected and standardized data is presented in Table 1. Experimental data, such as mode of action, assay, type of the cell and time of exposition are presented in Supplementary information file.

Structural descriptors

As it was previously reported, properties of released metal ions play a critical role in toxicity of metal oxide nanoparticles and are considered as essential to understand toxicity mechanism of MeOx NPs.[17,24,28–30] In this connection, several ionic characteristics were calculated: ionic radius (r), charge of metal ion (Z), electronegativity of metal (χ), covalent index (CI), cation polarizing power (CPP).[31] These parameters indirectly reflect the ability of metal ion to bind with biochemical ligands.[31,32] This includes interactions with protein-bonded sulfhydryl's or oxygen, as well as the process of depletion of glutathione.

Covalent index (CI) reflects the relative influence of covalent interactions in the binding process:

$$(CI) = \chi^2 \cdot r \quad (1)$$

Cation polarization power (CPP) indirectly reflects the relative importance of covalent interaction with bio-ligands:

$$(CPP) = \frac{Z^2}{r} \quad (2)$$

Previously it was also demonstrated, that intracellular redox state has a high influence on toxicity.[33,34] [4] Using thermodynamics equation, the band gap (E_g) was calculated

Table 1. Selected experimental toxicity data on various metal oxide nanoparticles

NP	E.C.[1] (№ 1)	E.C.[2] (№ 2)	E.C.[3] (№ 3)	E.C.[4] (№ 4)	H.[5]	P.P.[6]	A.[7] (№ 1)	A.[8] (№ 2)	C.[9] (№ 1)	C.[10] (№ 2)	B.[11] (№ 1)	B.[12] (№ 2)	P.S.[13]	T.T.[14]	V.F.[15]
Al_2O_3	2.49	2.42	2.75	2.31	1.85		3.01		3.01		3.01		3.31	3.01	3.01
Bi_2O_3	2.82	3.55	4.02		2.50										
CeO_2				2.54											
Co_3O_4				3.24		3.27	3.26	3.36	3.29	3.38	3.25	3.38	3.38	3.38	3.38
CoO	3.51	3.13	3.33	3.24	2.83										
Cr_2O_3	2.51	2.06	2.06	2.82	2.30	2.76									
CuO	3.20	4.24	5.71	3.31		2.32	3.62	3.32	3.80	2.90	3.83	3.86	5.20	5.05	4.75
Fe_2O_3	2.29	2.40	2.54	2.50	2.05	2.23									
Fe_3O_4				2.67		3.44	3.36		3.36		3.36		3.76	3.76	3.37
Gd_2O_3				2.86											
HfO_2				2.62											
In_2O_3	2.81	2.83	3.48	2.74	2.92										
La_2O_3	2.87	4.96	5.56	2.81	2.87										
MgO							2.60		2.60		2.60		2.60	2.60	2.60
Mn_2O_3				3.35	2.64										
Mn_3O_4							3.53	3.20	3.53	3.20	3.65	3.50	4.89	3.20	3.20
Nd_2O_3						2.93									
Ni_2O_3				2.96											
NiO	3.45	3.79	3.87	2.17	2.49	1.93									
Pr_6O_{11}						3.65									
Sb_2O_3	2.64	3.12	3.66	2.77	2.31		3.56	3.46	3.70	3.46	3.82	4.28	3.46	3.46	3.51
SiO_2	2.20	2.54	2.92	2.08	2.12		2.78		2.78		2.78		3.00	2.78	2.78
SnO_2	2.01	2.53	3.24	2.48	2.67										
TiO_2	1.74	2.14	4.68	2.20	1.76		2.90	2.90		2.90		2.90	4.60	3.03	2.90
V_2O_3	3.14	3.48	3.78		2.24										
WO_3				2.67	2.56	1.79	3.36		3.36		3.36		3.46	3.37	3.39
Y_2O_3	2.87	5.79	5.84	2.66	2.21										
Yb_2O_3				2.90											
ZnO	3.45	5.80	6.23	3.39	3.32	5.37	3.51	2.83	3.43		3.53	3.82	5.90	4.43	4.90
ZrO_2	2.15	2.58	3.04	2.39	2.02										

E.C.[1], E.C.[2], E.C.[3], E.C.[4] – cases for *Escherichia coli*; H.[5] – *HaCaT* cells; P.P.[6] - *Photobacterium phosphoreum*; A.[7], A.[8] – cases for A549 cells; C.[9], C.[10] – cases for Caco2 cells; B.[11], B.[12] – cases for Balb/c 3T3 cells; P.S.[13] – *Pseudokirchneriella subcapitata*; T.T.[14] – *Tetrahymena thermophile*; V.F.[15] – *Vibrio fischeri*.

using Portier's schema:[33,35]

$$E_{\Delta H^0} = \frac{-2 \cdot \Delta H_f^0 \cdot 2.612 \cdot 10^{19}}{N_A \cdot ne}, \quad (3)$$

where H_f^0 is the standard enthalpy of formation of the oxide, N_A is the Avogadro number; ne is the number of electrons transferred in the reaction. Then, the E_g is equal to:

$$E_g = A \cdot \exp(0.34 \cdot E_{\Delta H^0}) \quad (4)$$

The pre-exponential term A represents a property of the cation and it generally corresponds to a value of 1 for d-block elements, 0.8 for s-block elements, 1.35 for p-block elements and 0.5 for f-block elements.[33]

Other important properties for toxicity including some intrinsic characteristics, such as molecular mass of single metal oxide (MW), bulk density (ρ), and conditional radius of minimal interaction, Wigner-Seitz radius (r_w), were also established:[19,36]

$$r_w = \left(\frac{3 \cdot Mw}{4 \cdot \pi \cdot \rho \cdot N_A}\right)^{\frac{1}{3}} \quad (5)$$

where Mw – molecular weight; ρ – mass density.

Multi-task nano-read across

A general approach for proposed multi-task nano-read across modeling is similar to recently developed nano-read across techniques.[12,14,37] First, in this study the SOM model was generated. It the case of absence of reference nanoparticle (nanoparticle with known toxicity) in a certain group, a reference nanoparticle from the nearest group is selected. Based on available cytotoxicity information, the most accurate interspecies equation was selected. A Pearson correlation

coefficient for interspecies correlations (toxicity-toxicity correlations) was calculated to express relationships between different toxicities.[38,39] Missing data was estimated by scaling from the empirical data and calculated descriptors for a given endpoint. Toxicity-toxicity correlations and SOM model are combined via Gaussian distribution-based process modeling to fill data gaps.

Basically, SOM is the method related to a group of neural networks that use unsupervised learning.[17,40] Also, unsupervised learning does not see differences between dependent variables and endpoints. Unsupervised learning means that all variables are treated in the same way and there is no gold standard and no test checking procedure. Each SOM consists of a predefined number of neurons, where each neuron has an associated weight vector. The number of elements of each vector is equal to the dimensionality of the input space. In our case, we used 3×4 map. In SOM the identification of clusters corresponds to similar patterns of signaling pathway activity. It could be useful for the purpose of identification of common mechanisms of action for different types of nanoparticles.[34] In addition to identifying clusters, the SOM approach can aid in development of predictive quantitative structure-activity relations.[17]

All calculations discussed in this paper were performed using KNIME Analytics Platform.[41]

Results and discussion

The visual distribution of EC_{50} and IC_{50} values (including the minimal and maximal values) from Table 1 is represented in Figure 1. As it can be seen, the variance in data is not very high, however the highest variance is observed for CuO, La_2O_3 and ZnO (Figure 1).

We calculated the Pearson correlation coefficient for each pair of datasets to estimate their similarity (Table 2). Graphic representation of interspecies correlations is depicted in Figure 2. To evaluate the quality of obtained correlation, we used a common criterion, stating that the absolute value of Pearson correlation coefficient < 0.3 indicates a weak linear correlation between examined tests, absolute value in the range from 0.3 to 0.7 indicates the average relationship, and absolute value > 0.7 indicates a strong correlation.[42]

In most cases, toxicities measured in different tests demonstrate a strong correlation, for example: *E. coli* dataset №1 correlates well with *A549* cells dataset №1 (Person coefficient r = 0.824), with *Tetrahymena thermophile* dataset (r = 0.851), with *Vibrio fischeri* dataset (r = 0.926). Next, *E. coli* dataset №2 correlates well with *A549* dataset №1 (r = 0.735), with *Pseudokirchneriella subcapitata* dataset (r = 0.798), with *Tetrahymena thermophile* dataset (r = 0.821), with *Vibrio fischeri* dataset (r = 0.943). Third *E. coli* dataset correlates well with Caco2 dataset №2 (r = -0.869), with *Pseudokirchneriella subcapitata* dataset (r = 0.983), with *Tetrahymena thermophile* dataset (r = 0.839) and with *Vibrio fischeri* dataset (r = 0.864). All other connections are presented in Table 2. The strong linear correlation between examined tests suggests that toxic effects of nanomaterials are similar for these endpoints. This similarity may indicate that pattern of the toxic action is the same despite of utilized test type. Consequently, due to similarity, in this case one endpoint could be applied to predict toxic effect for other tests without necessity of experimental measurement.

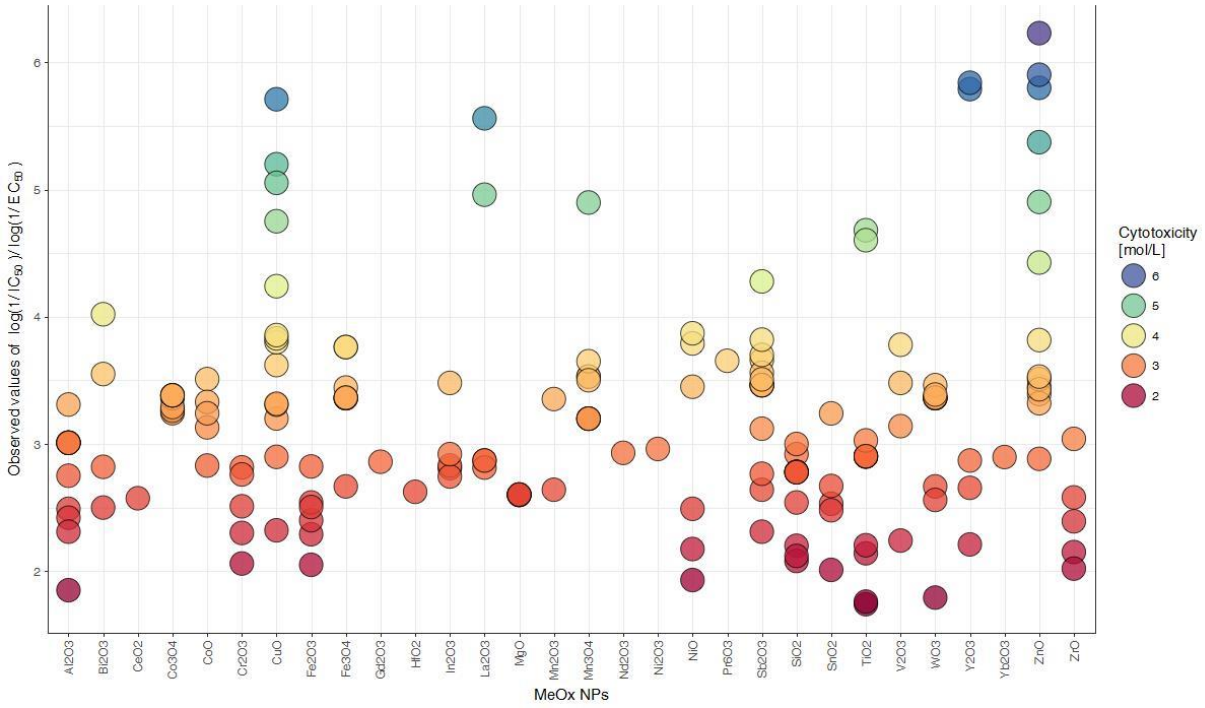

Figure 1. Range of cytotoxicity values for MeOx nanoparticles

Table 2. Interspecies correlations between toxicity datasets

	E.C.[1] (№1)	E.C.[2] (№ 2)	E.C.[3] (№ 3)	E.C.[4] (№ 4)	H.[5]	P.P.[6]	A.[7] (№ 1)	A.[8] (№ 2)	C.[9] (№ 1)	C.[10] (№ 2)	B.[11] (№ 1)	B.[12] (№ 2)	P.S.[13]	T.T.[14]
E.C.[2](№2)	**0.646**													
E.C.[3](№3)	0.425	**0.874**												
E.C.[4](№4)	**0.660**	0.521	0.470											
H.[5]	**0.647**	0.552	0.435	**0.725**										
P.P.[6]	0.237	**0.632**	0.496	0.586	**0.737**									
A.[7](№1)	**0.824**	**0.735**	**0.631**	**0.830**	**0.722**	0.010								
A.[8](№2)	0.097	-0.249	-0.576	0.180	-0.268	**-0.927**	0.437							
C.[9](№1)	**0.688**	0.524	**0.662**	**0.730**	0.499	-0.231	**0.983**	0.356						
C.[10](№2)	0.125	-0.047	**-0.869**	0.230	**0.999**	**0.999**	0.300	**0.702**	-0.523					
B.[11](№1)	**0.691**	**0.547**	**0.663**	**0.708**	0.518	-0.058	**0.982**	0.221	**0.993**	-0.400				
B.[12](№2)	**0.678**	0.451	-0.136	0.490	0.517	0.139	**0.863**	0.502	**0.692**	0.488	**0.747**			
P.S.[13]	**0.608**	**0.798**	**0.983**	0.588	**0.627**	0.586	**0.625**	**-0.714**	**0.674**	**-0.850**	**0.700**	-0.042		
T.T.[14]	**0.851**	**0.821**	**0.839**	**0.822**	**0.916**	0.198	**0.763**	-0.015	**0.761**	-0.397	**0.735**	0.489	**0.732**	
V.F.[15]	**0.926**	**0.943**	**0.864**	**0.867**	**0.934**	0.452	**0.749**	-0.162	**0.710**	-0.285	**0.704**	0.536	**0.779**	**0.955**

In bold are strong correlation measures.

As per common sense, the toxicity trends for the same species should be the same. However, in cases for *E. coli* datasets we found only average connection (0.425 < r < 0.660). We suggest that inconsistencies between datasets are related to different experimental conditions. For example, in the case of *E. coli* dataset №1, the duration of exposure was two hours in dark conditions[20] and for the case of *E. coli* datasets №2 and №3, the experiments were conducted under dark conditions and under light conditions, respectively.[21]

In the case of *E. coli* dataset №4 the duration of exposure was 24h under dark conditions.[22] At the same time, high correlation was observed for *E. coli* dataset №2 and *E. coli* dataset №3, where both tests were conducted for about 30 min under dark conditions and under light conditions, respectively).[21] It one more time confirms the importance of experimental conditions during the tests.

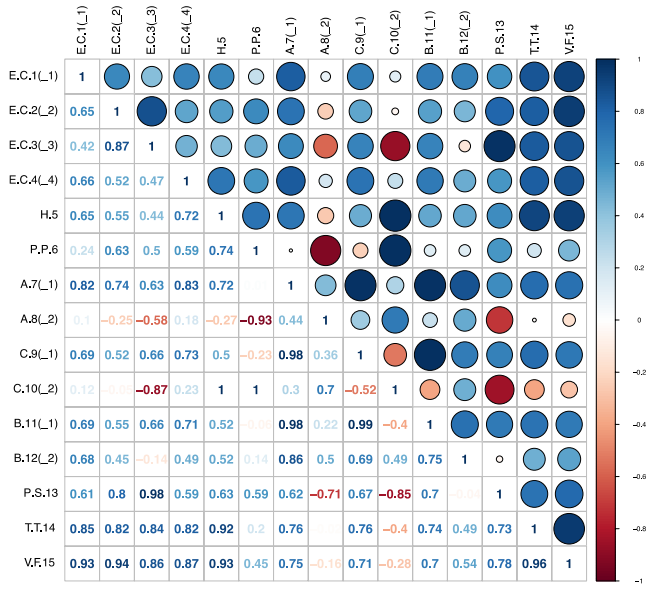

Figure 2. Interspecies correlations between toxicity datasets (based on Table 2)

The same situation was observed for *A549* cells (r = 0.437 for two datasets) and Caco2 cells (r = -0.523 for two datasets).[26,27] For those cases the exposure time was different: 12 hours and 24 hours, respectively.[26,27]

Initially nanoparticles were treated with fetal bovine serum, therefore we link inconsistencies in data to protein corona formation process. It is widely known, that the protein corona formation dramatically changes the toxicity of nanoparticles.[43,44]

In contrary, there was an agreement between *Balb/c 3T3* cells datasets (r = 0.747).[26,27] Two datasets for *Balb/c 3T3* cells were also treated 12 and 24 hours,[26,27] but all investigations were carried on the serum-free assay.

We found that the weakest connections were observed for different classes of bacteria, for instance, for *E. coli* dataset №1 and *Photobacterium phosphoreum* dataset (r = 0.237), *Photobacterium phosphoreum* dataset and *Vibrio fischeri* dataset (r = 0.452). In the case of *Photobacterium phosphoreum* and *Vibrio fischeri* which are members of same *Vibrionaceae* family, observed correlation can lead to misclassification. However, mentioned datasets share only 5 data points and only one of these points was anomalously different from the entire trend. We suppose that this amount of data is not sufficient to develop any trend for toxicity action.

From all 15 species, the bacteria *Photobacterium phosphoreum* shared the least number of strong connections. Eukaryotes (all cells, algal *Pseudokirchneriella subcapitata* and protozoa *Tetrahymena thermophile*) in most cases do demonstrate strong and average connections.

Above mentioned observations allow us to conclude that there are similar and dissimilar patterns of toxic action. The same nanoparticle may act in the similar way for different cells and bacteria, demonstrating similar patterns of the toxic action. However, some of mentioned trends are not representative, as some pairs shared data for small number of nanoparticles (less than 5 data points, see Table 1). Visualization of similar trends between metal oxide nanoparticles for different datasets is presented in Figure 3.

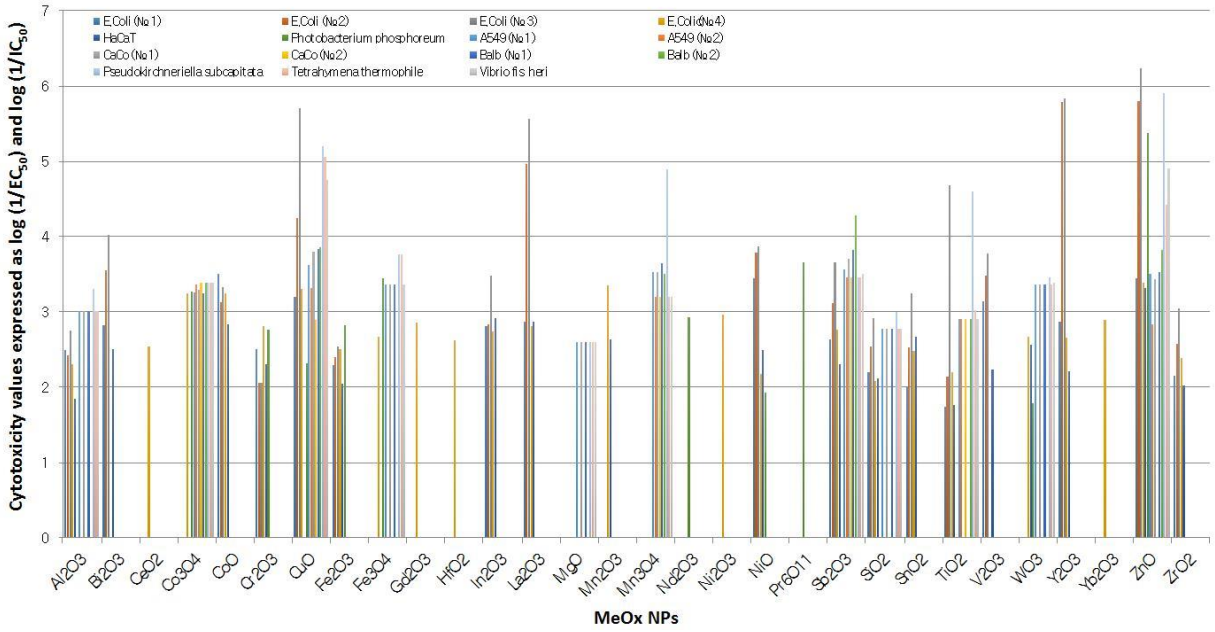

Figure 3. Trends of the cytotoxicity of MeOx nanoparticles towards different species

As it can be seen from Figure 2 and Figure 3, our results indicate that QSAR models developed in previous contributions[19,20,25,28,36,37] with some approximations are able to describe the cytotoxicity for different types of cells. To find possible links between nanoparticles in space of toxic responses, the SOM model was generated. Moreover, Figure 3 shows some interesting trends, confirming that most of the MeOx nanoparticles show similar cytotoxicity values for different types of cells.

For the purpose of SOM modeling the available toxicity data were utilized as descriptors. The best SOM model was chosen on the grounds of consistence with experimental data. The SOM representation (as two-dimensional projection) of the multidimensional data is presented in Figure 4. Although, we used the developed model to fill the gaps in the initial database. Results of predictions are presented in Table 3.

Analysis of the developed model revealed twelve groups of nanoparticles corresponding to four main risk categories (Figure 4): 1) non-toxic (green clusters, nanoparticles demonstrate low toxicity in all tests); 2) moderately hazardous (blue clusters, in some cases demonstrated toxicity); 3) highly hazardous (red clusters, nanoparticles demonstrate high toxicity in majority of tests); 4) imprecise (yellow cluster, nanoparticles demonstrate both low and high toxicity for different tests).

In overall, the SOM model consists of descriptors that relate to release of ion from the nanoparticle's surface (CI, CPP, etc). As it was demonstrated in our previous contribution, the most important outcome is the cause-effect relationships between the enthalpy of cation's formation and toxicity.[28] At the same time, the enthalpy has a clear connection with ion's charge and CPP and those descriptors indirectly describe the same processes. Since the calculations presented in current paper are simpler and faster when compared with the computation of enthalpy, it might be more efficient instead of enthalpy to use ion charge and CPP in modeling the toxicity.

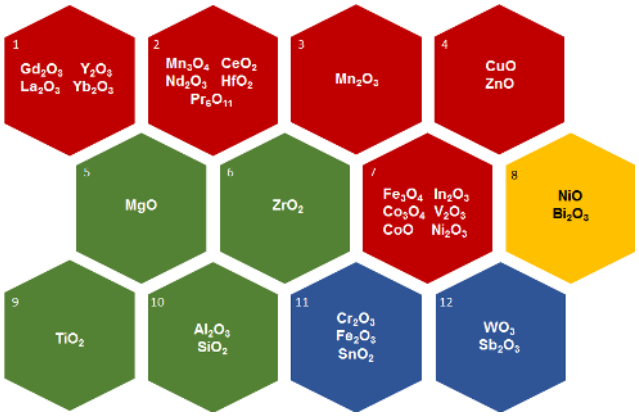

Figure 4. A representation of similarity in toxicity between MeOx nanoparticles applying SOM clustering technique

Table 3. Toxicity data with additional number obtained by applying the suggested methodology to fill experimental gaps

NP	E.C.[1]	E.C.[2]	E.C.[3]	E.C.[4]	H.[5]	P.P.[6]	A.[7]	A.[8]	C.[9]	C.[10]	B.[11]	B.[12]	P.S.[13]	T.T.[14]	V.F.[15]
Al_2O_3	2.49	2.42	2.75	2.31	1.85	**out**	3.01	**3.21**	3.01	**out**	3.01	**out**	3.31	3.01	3.01
Bi_2O_3	2.82	3.55	4.02	**2.76**	2.50	**2.16**	**3.42**	**3.39**	**3.48**	**3.38**	**3.50**	**4.01**	**3.36**	**3.52**	**3.39**
CeO_2	**2.49**	**3.43**	**4.09**	2.54	**2.48**	**2.89**	**3.20**	**3.02**	**3.33**	**3.08**	**3.37**	**3.39**	**4.14**	**3.30**	**3.27**
Co_3O_4	**2.89**	**3.36**	**3.73**	3.24	**2.57**	3.27	3.26	3.36	3.29	3.38	3.25	3.38	3.38	3.38	3.38
CoO	3.51	3.13	3.33	3.24	2.83	**3.06**	**3.36**	**3.25**	**3.32**	**3.25**	**3.35**	**3.95**	**4.09**	**3.89**	**3.94**
Cr_2O_3	2.51	2.06	2.06	2.82	2.30	2.76	**3.40**	**3.30**	**3.46**	**3.28**	**3.50**	**3.76**	**3.93**	**3.59**	**3.56**
CuO	3.20	4.24	5.71	3.31	**2.73**	2.32	3.62	3.32	3.8	2.90	3.83	3.86	5.20	5.05	4.75
Fe_2O_3	2.29	2.40	2.54	2.50	2.05	2.82	**3.35**	**3.30**	**3.46**	**3.25**	**3.50**	**3.81**	**3.81**	**3.57**	**3.48**
Fe_3O_4	**2.80**	**3.48**	**3.99**	2.67	**2.52**	3.44	3.36	**3.27**	3.36	**3.30**	3.36	**3.77**	3.76	3.76	3.37
Gd_2O_3	**2.71**	**out**	**out**	2.86	**2.37**	**2.87**	**3.19**	**3.16**	**3.27**	**3.25**	**3.31**	**3.69**	**3.77**	**3.04**	**2.97**
HfO_2	**2.48**	**out**	**out**	2.62	**2.45**	**2.19**	**3.21**	**3.10**	**3.26**	**3.11**	**3.28**	**3.28**	**3.98**	**3.29**	**3.28**
In_2O_3	2.81	2.83	3.48	2.74	2.92	**2.75**	**3.39**	**3.26**	**3.43**	**3.32**	**3.46**	**3.82**	**3.83**	**3.53**	**3.50**
La_2O_3	2.87	4.96	5.56	2.81	2.87	**3.47**	**3.22**	**3.07**	**3.31**	**3.22**	**3.36**	**3.69**	**4.09**	**3.18**	**3.17**
MgO	**out**	**out**	**out**	**2.80**	**2.66**	**out**	2.60	**3.12**	2.60	**out**	2.60	**out**	2.60	2.60	2.60
Mn_2O_3	**2.72**	**3.49**	**out**	3.35	2.64	**out**	**3.23**	**3.15**	**3.24**	**3.22**	**out**	**out**	**out**	**out**	**out**
Mn_3O_4	**2.75**	**3.65**	**4.13**	**2.74**	**2.22**	**3.27**	3.53	3.20	3.53	3.20	3.65	3.50	4.90	3.20	3.20
Nd_2O_3	**2.73**	**3.91**	**4.35**	**2.86**	**2.52**	2.93	**3.30**	**3.15**	**3.43**	**3.20**	**3.47**	**3.67**	**3.94**	**3.28**	**3.18**
Ni_2O_3	**2.71**	**3.21**	**3.83**	2.96	**2.50**	**3.33**	**3.35**	**3.20**	**3.39**	**3.17**	**3.43**	**3.52**	**4.09**	**3.591**	**3.59**
NiO	3.45	3.79	3.87	2.17	2.49	1.93	**3.34**	**3.33**	**3.31**	**3.20**	**3.34**	**4.00**	**3.94**	**3.86**	**3.82**
Pr_6O_{11}	**3.04**	**4.92**	**4.90**	**3.21**	**2.54**	3.65	**3.63**	**3.41**	**3.72**	**3.55**	**3.78**	**3.99**	**3.51**	**3.01**	**2.80**
Sb_2O_3	2.64	3.12	3.66	2.77	2.31	**2.37**	3.56	3.46	3.70	3.46	3.82	4.28	3.46	3.46	3.51
SiO_2	2.20	2.54	2.92	2.08	2.12	**3.50**	2.78	**3.14**	2.78	**3.39**	2.78	**3.20**	3.00	2.78	2.78
SnO_2	2.01	2.53	3.24	2.48	2.67	**2.39**	**3.27**	**3.22**	**out**	**out**	**out**	**out**	**out**	**out**	**out**
TiO_2	1.74	2.14	4.68	2.20	1.76	**3.35**	2.90	2.90	**3.48**	2.90	**3.52**	2.90	4.60	3.03	2.90
V_2O_3	3.14	3.48	3.78	**2.86**	2.24	**3.34**	**3.40**	**3.16**	**3.45**	**3.17**	**3.49**	**3.54**	**4.32**	**3.61**	**3.63**
WO_3	**1.82**	**1.40**	**2.65**	2.67	2.56	1.79	3.36	**3.21**	3.36	**3.17**	3.36	**2.86**	3.46	3.37	3.39
Y_2O_3	2.87	5.79	5.84	2.66	2.21	**3.56**	**3.11**	**3.07**	**3.19**	**3.16**	**3.24**	**3.66**	**4.09**	**3.09**	**3.09**
Yb_2O_3	**2.73**	**4.05**	**4.23**	2.90	**2.42**	**2.49**	**3.23**	**3.18**	**3.27**	**3.24**	**3.31**	**3.58**	**3.81**	**3.08**	**3.02**
ZnO	3.45	5.80	6.23	3.39	3.32	5.37	3.51	2.83	3.43	**3.11**	3.53	3.82	5.90	4.43	4.90
ZrO_2	2.15	2.58	3.04	2.39	2.02	**2.78**	**3.20**	**3.09**	**out**	**out**	**out**	**out**	**out**	**3.27**	**out**

Predicted values are in bold

Even though there are similar patterns of action in different species, differences in exposure scenarios may still exist for different cells or organisms. For instance, it is clear that eukaryotes and prokaryotes handle the uptake of metal ions in different ways.[19,45] Let us discuss each cluster and potential scenarios in detail.

In general, five major mechanisms of nanoparticles' toxicity are reported: 1) direct damages by released ions, such as DNA induction or depletion of glutathione and bonding to sulfhydryl or oxygen-containing groups of proteins; 2) oxidative stress induced by excessive production of reactive forms of oxygen by released ions or surface of nanoparticle; 3) adsorption of biologically active molecules onto nanoparticle's surface; 4) molecular structure related effects (due to band gap or crystalline form) that result in photochemical and redox properties; and 5) Trojan horse effects.[19,33,46–48]

Red group (clusters 1, 2, 3, 4 and 7) could be divided among three subsets: subset with cluster 1, subset with clusters 2, 3, 7, and subset with cluster 4, respectively.

As per cluster 4, that included ZnO and CuO nanoparticles, the lethal genotoxic responses were associated with release of ions and high solubility of nanoparticles (mechanisms № 1 and № 2).[17,26,32]

Certain amount of both Cu^{2+} and Zn^{2+} is necessary for biological function; therefore, the balance between intracellular and extracellular contents of these ions is regulated at the cellular level. However, increasing concentration of ions entering the cell will result in increasing toxicity. Similar outcomes were reported by other researchers.[49,50] Next, cytotoxicity of Zn^{2+} and Cu^{2+} comes from the fact, that copper ions are prone to participate in the formation of reactive oxygen species via Fenton reaction.[19]

According to Nieboer, metal ions from clusters 1, 2 and 3 are oxygen-seeking (mechanism № 1).[31] Nanoparticles Gd_2O_3, Y_2O_3, Yb_2O_3 and La_2O_3 in cluster 1 belong to group 3 in the periodic table of elements. Cluster 1 shares similar values of standard reduction potential in reaction $Me^{x+} + x\bar{e} \leftrightarrow Me^0$: -2.279 for Gd^{3+}, -2.379 for La^{3+}, -2.372 for Y^{3+} and -2.19 for Yb^{3+} (mechanism № 4). Next group 2 also contains three lanthanides CeO_2, Nd_2O_3, Pr_6O_{11} and two transition-metal oxides HfO_2 and Mn_3O_4. Third cluster includes only Mn_2O_3 nanoparticle.

Cluster 7 grouped Fe_3O_4, Co_3O_4, CoO, In_2O_3, V_2O_3 and Ni_2O_3 nanoparticles. Ivask *et al.* supposed that toxic effects of Mn_3O_4 and Co_3O_4 could be attributed to the ROS-inducing ability of surface or released ions (mechanisms № 1 and № 2).[26] In this group, Fe_3O_4, CoO and In_2O_3 could be moderately soluble (mechanism № 1).[17,46,51] It was found that vanadium and cobalt can undergo redox-cycling reactions (mechanism № 4).[47]

As it can be seen from the Figure 3, TiO_2, MgO, ZrO_2, Al_2O_3 and SiO_2 (clusters 5, 6, 9, 10) were grouped as safe nanomaterials. These results are in agreement with current theories of nanotoxicology.[52–54] The remarkable fact is that all mentioned nanoparticles are safe for different species. In the case of cluster 10 (Figure 3), results were identical to previously developed cheminformatics model as it was earlier demonstrated by *Rallo et al.*[17] In mentioned contribution, safe responses to Al_2O_3 and SiO_2 nanoparticles were related to the low production rate of ROS. ZrO_2 from cluster 6 and TiO_2 from cluster 9 are the most insoluble oxides (mechanism №1).

In seems that diverse toxicities of species in cluster 8 (NiO, Bi_2O_3) were related to differences of the natural resistance of different organisms/cells. For instance, NiO demonstrated high toxicity towards *E. coli*, but toxicity towards *HaCaT* cells and *Photobacterium phosphoreum* were low.[21,23,25] Nickel replaces the essential metal of metalloproteins in *E. coli*, inducing the toxicity.[55] At the same time, *Photobacterium phosphoreum* is nikel-tolerant.[56] In the case of cells (*HaCaT* cells, Table 1), Ni^{2+} produces rather low, but measurable levels of free radicals.[57] Both NiO and Bi_2O_3 are moderately soluble, which may lead to release of ions and production of ROS (mechanisms №1 and 2). In the case of Zebrafish (unstudied in current paper) it has been proven that soluble NiO evokes the formation of free radicals (mechanism № 2).[49]

Nanoparticles from the cluster 11 (Fe_2O_3, Cr_2O_3 and SnO_2) are preferably stable and could release ions that demonstrate borderline pattern of action in terms of ionic behavior.[31] Ions of iron and chromium can undergo redox-cycling reactions (mechanism № 4).[47] Fe^{3+} and Cr^{3+} are normally present in cell cycle, the balance between intracellular and extracellular contents of these ions is regulated. As the solubility of these ions is moderate, this balance remains stable (mechanism № 1).

Nanoparticles in cluster 12 are low toxic. WO_3 is chemically inert and stable in aqueous media over a very wide pH range.[58] Low solubility could be the reason why WO_3 and Sb_2O_3 from cluster 12 do not gain an access to the reactive cites in cells (mechanism №1).[31]

As one can see from Table 3, in some cases, predicted values were out of the applicability domain. It could be explained by lack of certain cases (values of toxicity) in initial database, that limited predictive ability of developed space of descriptors.

Conclusions

In this study, we have presented a comprehensive, predictive multi-nano-read-across model of metal oxide nanoparticles' toxicity. Using the developed approach, we have analysed hidden patterns of multidimensional toxicological data and found the similarity within datasets. All nanoparticles were categorized to four main patterns of nanotoxicological action. Based on similarity of toxic action, we have estimated the cytotoxicity for experimentally untested nano-sized metal oxides. Presented approach provides both qualitative and quantitative categorization of nanoparticles towards different cells and bacteria. Developed model also reveals the differences in the mechanisms of toxicity of metal oxide nanoparticles towards different prokaryotes and eukaryotes. The mechanistic insight of the developed models lies within known theories of nanotoxicity.

We also demonstrated that it is very important to have data that measured at same conditions. However, variation of endpoints due to different experimental conditions does not abrogate the same pattern of action of nanomaterials. Using similarity measures we found and discussed differences in the mechanisms of toxic action of nanoparticles for prokaryotes and eukaryotes.

The proposed combined approach may be helpful to broaden knowledge on toxicity of nanomaterials and can be used for safe-by-design approach. Developed multi-nano-read-across approach could be beneficial for cross-species prediction of toxicity of nano-sized metal oxides as well as a useful tool for early risk assessment of metal oxide nanoparticles.

Conflicts of Interest

There are no conflicts to declare.

Acknowledgements

The authors thank for support of the NSF CREST Interdisciplinary Nanotoxicity Center NSF-CREST - Grant # HRD-0833178. This work is supported in part by the NSF under ND EPSCoR Award #IIA-1355466 and by the State of North Dakota.

Notes and references

1 P. Couvreur and C. Vauthier, *Pharm. Res.*, 2006, **23**, 1417.
2 M. J. Ellenbecker and C. S.-J. Tsai, in *Exposure Assessment and Safety Considerations for Working with Engineered Nanoparticles*, John Wiley & Sons, Inc, 2015, pp. 28–38.
3 H. Bahadar, F. Maqbool, K. Niaz and M. Abdollahi, 2016, *Iran. Biomed. J.*, **20**, 1.
4 A. E. Nel, *J. Intern. Med.*, 2013, **274**, 561.
5 V. C. Epa, F. R. Burden, C. Tassa, R. Weissleder, S. Shaw and D. A. Winkler, *Nano Lett.*, 2012, **12**, 5808.
6 V. Maojo, M. Fritts, F. Martin-Sanchez, D. la Iglesia, R. E. Cachau, M. Garcia-Remesal, J. Crespo, J. A. Mitchell, A.

Anguita, N. Baker, J. M. Barreiro, S. E. Benitez, G. la Calle, J. C. Facelli, P. Ghazal, A. Geissbuhler, F. Gonzalez-Nilo, N. Graf, P. Grangeat, I. Hermosilla, R. Hussein, J. Kern, S. Koch, Y. Legre, V. Lopez-Alonso, G. Lopez-Campos, L. Milanesi, V. Moustakis, C. Munteanu, P. Otero, A. Pazos, D. Perez-Rey, G. Potamias, F. Sanz and C. Kulikowski, *Computing*, 2012, **94**, 521.
7 N. Sizochenko and J. Leszczynski, *J. Nanotoxicology Nanomedicine*, 2016, **1**, 1.
8 R. Tantra, C. Oksel, T. Puzyn, J. Wang, K. N. Robinson, X. Z. Wang, C. Y. Ma and T. Wilkins, *Nanotoxicology*, 2015, **9**, 636.
9 V. V Kleandrova, F. Luan, H. González-Díaz, J. M. Ruso, A. Speck-Planche and M. N. D. S. Cordeiro, *Environ. Sci. Technol.*, 2014, **48**, 14686.
10 N. Sizochenko, B. Rasulev, A. Gajewicz, E. Mokshyna, V. E. Kuz'min, J. Leszczynski and T. Puzyn, *RSC Adv.*, 2015, **5**, 77739.
11 OECD, *Approaches on nano grouping/ equivalence/read-across concepts based on physical-chemical properties (gera-pc) for regulatory regimes.*, 2016.
12 G. A. Oomen, A. E. Bleeker, M. P. Bos, F. van Broekhuizen, S. Gottardo, M. Groenewold, D. Hristozov, K. Hund-Rinke, M.-A. Irfan, A. Marcomini, J. W. Peijnenburg, K. Rasmussen, S. A. Jiménez, J. J. Scott-Fordsmand, M. van Tongeren, K. Wiench, W. Wohlleben and R. Landsiedel, *Int. J. Environ. Res. Public Heal.,* 2015, **12**, 13415.
13 A. Gajewicz, M. T. D. Cronin, R. Bakhtiyor, L. Jerzy and T. Puzyn, *Nanotechnology*, 2015, **26**, 15701.
14 J. H. E. Arts, M. Hadi, A. M. Keene, R. Kreiling, D. Lyon, M. Maier, K. Michel, T. Petry, U. G. Sauer, D. Warheit, K. Wiench and R. Landsiedel, *Regul. Toxicol. Pharmacol.*, 2014, **70**, 492.
15 N. Fjodorova, M. Novic, A. Gajewicz and B. Rasulev, *Nanotoxicology*, 2017, 11, 475.
16 M. Saar-Tsechansky and F. Provost, *J. Mach. Learn. Res.*, 2007, **8**, 1623.
17 R. Rallo, B. France, R. Liu, S. Nair, S. George, R. Damoiseaux, F. Giralt, A. Nel, K. Bradley and Y. Cohen, *Environ. Sci. Technol.*, 2011, **45**, 1695.
18 R. Liu, B. France, S. George, R. Rallo, H. Zhang, T. Xia, A. E. Nel, K. Bradley and Y. Cohen, *Analyst*, 2014, **139**, 943.
19 N. Sizochenko, B. Rasulev, A. Gajewicz, V. Kuz'min, T. Puzyn and J. Leszczynski, *Nanoscale*, 2014, **6**, 13986.
20 T. Puzyn, B. Rasulev, A. Gajewicz, X. Hu, T. P. Dasari, A. Michalkova, H.-M. Hwang, A. Toropov, D. Leszczynska and J. Leszczynski, *Nat. Nanotechnol.*, 2011, **6**, 175.
21 K. Pathakoti, M.-J. Huang, J. D. Watts, X. He and H.-M. Hwang, *J. Photochem. Photobiol. B Biol.*, 2014, **130**, 234.
22 C. Kaweeteerawat, A. Ivask, R. Liu, H. Zhang, C. H. Chang, C. Low-Kam, H. Fischer, Z. Ji, S. Pokhrel, Y. Cohen, D. Telesca, J. Zink, L. Mädler, P. A. Holden, A. Nel and H. Godwin, *Environ. Sci. Technol.*, 2015, **49**, 1105.
23 D. Wang, Y. Gao, Z. Lin, Z. Yao and W. Zhang, *Aquat. Toxicol.*, 2014, **154**, 200.
24 V. Aruoja, S. Pokhrel, M. Sihtmae, M. Mortimer, L. Madler and A. Kahru, *Environ. Sci. Nano*, 2015, **2**, 630–644.
25 A. Gajewicz, N. Schaeublin, B. Rasulev, S. Hussain, D. Leszczynska, T. Puzyn and J. Leszczynski, *Nanotoxicology*, 2015, **9**, 313.
26 A. Ivask, T. Titma, M. Visnapuu, H. Vija, A. Kakinen, M. Sihtmae, S. Pokhrel, L. Madler, M. Heinlaan, V. Kisand and R. S. and A. Kahru, *Curr. Top. Med. Chem.*, 2015, 15, 1914.
27 T. Titma, R. Shimmo, J. Siigur and A. Kahru, *Cytotechnology*, 2016, **68**, 2363.
28 N. Sizochenko, A. Gajewicz, J. Leszczynski and T. Puzyn, *Nanoscale*, 2016, **8**, 7203.
29 W.-S. Cho, R. Duffin, F. Thielbeer, M. Bradley, I. L. Megson, W. MacNee, C. A. Poland, C. L. Tran and K. Donaldson, *Toxicol. Sci.*, 2012, **126**, 469.
30 C. C. Chusuei, C.-H. Wu, S. Mallavarapu, F. Y. S. Hou, C.-M. Hsu, J. G. Winiarz, R. S. Aronstam and Y.-W. Huang, *Chem. Biol. Interact.*, 2013, **206**, 319.
31 E. Nieboer and D. H. S. Richardson, *Environ. Pollut. Ser. B, Chem. Phys.*, 1980, **1**, 3.
32 C. P. Tatara, M. C. Newman, J. T. McCloskey and P. L. Williams, *Aquat. Toxicol.*, 1998, **42**, 255.
33 E. Burello and A. P. Worth, *Nanotoxicology*, 2011, **5**, 228–235.
34 S. George, T. Xia, R. Rallo, Y. Zhao, Z. Ji, S. Lin, X. Wang, H. Zhang, B. France, D. Schoenfeld, R. Damoiseaux, R. Liu, S. Lin, K. A. Bradley, Y. Cohen and A. E. Nel, *ACS Nano*, 2011, **5**, 1805.
35 J. Portier, H. S. Hilal, I. Saadeddin, S. J. Hwang, M. A. Subramanian and G. Campet, *Prog. Solid State Chem.*, 2004, **32**, 207.
36 S. Kar, A. Gajewicz, T. Puzyn, K. Roy and J. Leszczynski, *Ecotoxicol. Environ. Saf.*, 2014, **107**, 162.
37 A. Gajewicz, K. Jagiello, M. T. D. Cronin, J. Leszczynski and T. Puzyn, *Environ. Sci. Nano*, 2017, **4**, 346.
38 K. L. E. Kaiser, M. B. McKinnon and F. L. Fort, *Environ. Toxicol. Chem.*, 1994, **13**, 1599.
39 J. Devillers and H. Devillers, *SAR QSAR Environ. Res.*, 2009, **20**, 467–500.
40 M. M. Van Hulle, eds. G. Rozenberg, T. Bäck and J. N. Kok, Springer Berlin Heidelberg, Berlin, Heidelberg, 2012, pp. 585.
41 M. R. Berthold, *SIGKDD Explor.*, 2009, **11**, 26.
42 B. Dunn, M. Mørreaunet and Y. Roudi, *PLOS Comput. Biol.*, 2015, **11**, e1004052.
43 T. Cedervall, I. Lynch, S. Lindman, T. Berggård, E. Thulin, H. Nilsson, K. A. Dawson and S. Linse, *Proc. Natl. Acad. Sci.*, 2007, **104**, 2050.
44 R. Liu, W. Jiang, C. D. Walkey, W. C. W. Chan and Y. Cohen, *Nanoscale*, 2015, **7**, 9664.
45 J. A. Lemire, J. J. Harrison and R. J. Turner, *Nat Rev Micro*, 2013, **11**, 371.
46 H. Zhang, Z. Ji, T. Xia, H. Meng, C. Low-Kam, R. Liu, S. Pokhrel, S. Lin, X. Wang, Y.-P. Liao, M. Wang, L. Li, R. Rallo, R. Damoiseaux, D. Telesca, L. Mädler, Y. Cohen, J. I. Zink and A. E. Nel, *ACS Nano*, 2012, **6**, 4349.
47 M. Valko and H. M. and M. T. D. Cronin, *Curr. Med. Chem.*, 2005, 12, 1161.
48 I. Lynch, C. Weiss and E. Valsami-Jones, *Nano Today*, 2014, **9**, 266.
49 S. Lin, Y. Zhao, Z. Ji, J. Ear, C. H. Chang, H. Zhang, C. Low-Kam, K. Yamada, H. Meng, X. Wang, R. Liu, S. Pokhrel, L. Mädler, R. Damoiseaux, T. Xia, H. A. Godwin, S. Lin and A. E. Nel, *Small*, 2013, **9**, 1776.
50 E. Papa, J. P. Doucet and A. Doucet-Panaye, *SAR QSAR Environ. Res.*, 2015, **26**, 647.
51 B. Harper, D. Thomas, S. Chikkagoudar, N. Baker, K. Tang, A. Heredia-Langner, R. Lins and S. Harper, *J. Nanopart. Res.*, 2015, **17**, 250.
52 G. Oberdörster, E. Oberdörster and J. Oberdörster, *Environ. Health Perspect.*, 2005, **113**, 823–839.
53 L. Gonzalez, D. Lison and M. Kirsch-Volders, *Nanotoxicology*, 2008, **2**, 252.
54 S. Y. Shaw, E. C. Westly, M. J. Pittet, A. Subramanian, S. L. Schreiber and R. Weissleder, *Proc. Natl. Acad. Sci.*, 2008, **105**, 7387.
55 L. Macomber and R. P. Hausinger, *Metallomics*, 2011, **3**, 1153.
56 Y. Zeng, L. Wang, L. Jiang, X. Cai and Y. Li, *Bull. Environ. Contam. Toxicol.*, 2015, **95**, 260.
57 J. Weaver, S. Porasuphatana, P. Tsai, G.-L. Cao, T. A. Budzichowski, L. J. Roman and G. M. Rosen, *Toxicol. Sci.*, 2004, **81**, 325.
58 A. Kahru and A. Ivask, *Acc. Chem. Res.*, 2013, **46**, 823.

Supporting Information

How toxicity of nanomaterials towards different species could be simultaneously evaluated: Novel multi-nano-read-across approach

Natalia Sizochenko,[a,b,c] Alicja Mikolajczyk,[a,b] Karolina Jagiello,[a] †
Tomasz Puzyn,[a] Jerzy Leszczynski[b†] and Bakhtiyor Rasulev[b,c]

a. Laboratory of Environmental Chemometrics, Institute for Environmental and Human Health Protection, Faculty of Chemistry, University of Gdansk, Gdansk, Poland.
b. Interdisciplinary Nanotoxicity Center, Department of Chemistry and Biochemistry, Jackson State University, Jackson MS, USA.
c. Department of Coatings and Polymeric Materials, North Dakota State University, Fargo, ND, USA.

†corresponding authors:
jerzy@icnanotox.org
bakhtiyor.rasulev@ndsu.edu

Nanoparticle	Mode of action	Assay	Type of the cell	Time of exposition	Notes
Al2O3	viability test	Minimum Inhibitory Concentration Assay	Escherichia coli	2 hours	dark conditions
Bi2O3	viability test	Minimum Inhibitory Concentration Assay	Escherichia coli	2 hours	dark conditions
CoO	viability test	Minimum Inhibitory Concentration Assay	Escherichia coli	2 hours	dark conditions
Cr2O3	viability test	Minimum Inhibitory Concentration Assay	Escherichia coli	2 hours	dark conditions
CuO	viability test	Minimum Inhibitory Concentration Assay	Escherichia coli	2 hours	dark conditions
Fe2O3	viability test	Minimum Inhibitory Concentration Assay	Escherichia coli	2 hours	dark conditions
In2O3	viability test	Minimum Inhibitory Concentration Assay	Escherichia coli	2 hours	dark conditions
La2O3	viability test	Minimum Inhibitory Concentration Assay	Escherichia coli	2 hours	dark conditions
NiO	viability test	Minimum Inhibitory Concentration Assay	Escherichia coli	2 hours	dark conditions
Sb2O3	viability test	Minimum Inhibitory Concentration Assay	Escherichia coli	2 hours	dark conditions
SiO2	viability test	Minimum Inhibitory Concentration Assay	Escherichia coli	2 hours	dark conditions
SnO2	viability test	Minimum Inhibitory Concentration Assay	Escherichia coli	2 hours	dark conditions
TiO2	viability test	Minimum Inhibitory Concentration Assay	Escherichia coli	2 hours	dark conditions
V2O3	viability test	Minimum Inhibitory Concentration Assay	Escherichia coli	2 hours	dark conditions
Y2O3	viability test	Minimum Inhibitory Concentration Assay	Escherichia coli	2 hours	dark conditions
ZnO	viability test	Minimum Inhibitory Concentration Assay	Escherichia coli	2 hours	dark conditions
ZrO2	viability test	Minimum Inhibitory Concentration Assay	Escherichia coli	2 hours	dark conditions
Al2O3	viability test	Minimum Inhibitory Concentration Assay	Escherichia coli	30 minutes	dark conditions
Bi2O3	viability test	Minimum Inhibitory Concentration Assay	Escherichia coli	30 minutes	dark conditions
CoO	viability test	Minimum Inhibitory Concentration Assay	Escherichia coli	30 minutes	dark conditions
Cr2O3	viability test	Minimum Inhibitory Concentration Assay	Escherichia coli	30 minutes	dark conditions
CuO	viability test	Minimum Inhibitory Concentration Assay	Escherichia coli	30 minutes	dark conditions
Fe2O3	viability test	Minimum Inhibitory Concentration Assay	Escherichia coli	30 minutes	dark conditions
In2O3	viability test	Minimum Inhibitory Concentration Assay	Escherichia coli	30 minutes	dark conditions
La2O3	viability test	Minimum Inhibitory Concentration Assay	Escherichia coli	30 minutes	dark conditions
NiO	viability test	Minimum Inhibitory Concentration Assay	Escherichia coli	30 minutes	dark conditions
Sb2O3	viability test	Minimum Inhibitory Concentration Assay	Escherichia coli	30 minutes	dark conditions
SiO2	viability test	Minimum Inhibitory Concentration Assay	Escherichia coli	30 minutes	dark conditions
SnO2	viability test	Minimum Inhibitory Concentration Assay	Escherichia coli	30 minutes	dark conditions
TiO2	viability test	Minimum Inhibitory Concentration Assay	Escherichia coli	30 minutes	dark conditions
V2O3	viability test	Minimum Inhibitory Concentration Assay	Escherichia coli	30 minutes	dark conditions
Y2O3	viability test	Minimum Inhibitory Concentration Assay	Escherichia coli	30 minutes	dark conditions
ZnO	viability test	Minimum Inhibitory Concentration Assay	Escherichia coli	30 minutes	dark conditions
ZrO2	viability test	Minimum Inhibitory Concentration Assay	Escherichia coli	30 minutes	dark conditions
Al2O3	viability test	Minimum Inhibitory Concentration Assay	Escherichia coli	30 minutes	photo-induced conditions
Bi2O3	viability test	Minimum Inhibitory Concentration Assay	Escherichia coli	30 minutes	photo-induced conditions
CoO	viability test	Minimum Inhibitory Concentration Assay	Escherichia coli	30 minutes	photo-induced conditions
Cr2O3	viability test	Minimum Inhibitory Concentration Assay	Escherichia coli	30 minutes	photo-induced conditions
CuO	viability test	Minimum Inhibitory Concentration Assay	Escherichia coli	30 minutes	photo-induced conditions
Fe2O3	viability test	Minimum Inhibitory Concentration Assay	Escherichia coli	30 minutes	photo-induced conditions
In2O3	viability test	Minimum Inhibitory Concentration Assay	Escherichia coli	30 minutes	photo-induced conditions
La2O3	viability test	Minimum Inhibitory Concentration Assay	Escherichia coli	30 minutes	photo-induced conditions
NiO	viability test	Minimum Inhibitory Concentration Assay	Escherichia coli	30 minutes	photo-induced conditions
Sb2O3	viability test	Minimum Inhibitory Concentration Assay	Escherichia coli	30 minutes	photo-induced conditions
SiO2	viability test	Minimum Inhibitory Concentration Assay	Escherichia coli	30 minutes	photo-induced conditions
SnO2	viability test	Minimum Inhibitory Concentration Assay	Escherichia coli	30 minutes	photo-induced conditions
TiO2	viability test	Minimum Inhibitory Concentration Assay	Escherichia coli	30 minutes	photo-induced conditions
V2O3	viability test	Minimum Inhibitory Concentration Assay	Escherichia coli	30 minutes	photo-induced conditions
Y2O3	viability test	Minimum Inhibitory Concentration Assay	Escherichia coli	30 minutes	photo-induced conditions
ZnO	viability test	Minimum Inhibitory Concentration Assay	Escherichia coli	30 minutes	photo-induced conditions
ZrO2	viability test	Minimum Inhibitory Concentration Assay	Escherichia coli	30 minutes	photo-induced conditions
Al2O3	growth inhibition	Minimum Inhibitory Concentration Assay	Escherichia coli	24 hours	dark conditions
CeO2	growth inhibition	Minimum Inhibitory Concentration Assay	Escherichia coli	24 hours	dark conditions
Co3O4	growth inhibition	Minimum Inhibitory Concentration Assay	Escherichia coli	24 hours	dark conditions
CoO	growth inhibition	Minimum Inhibitory Concentration Assay	Escherichia coli	24 hours	dark conditions
Cr2O3	growth inhibition	Minimum Inhibitory Concentration Assay	Escherichia coli	24 hours	dark conditions
CuO	growth inhibition	Minimum Inhibitory Concentration Assay	Escherichia coli	24 hours	dark conditions
Fe2O3	growth inhibition	Minimum Inhibitory Concentration Assay	Escherichia coli	24 hours	dark conditions
Fe3O4	growth inhibition	Minimum Inhibitory Concentration Assay	Escherichia coli	24 hours	dark conditions
Gd2O3	growth inhibition	Minimum Inhibitory Concentration Assay	Escherichia coli	24 hours	dark conditions
HfO2	growth inhibition	Minimum Inhibitory Concentration Assay	Escherichia coli	24 hours	dark conditions
In2O3	growth inhibition	Minimum Inhibitory Concentration Assay	Escherichia coli	24 hours	dark conditions
La2O3	growth inhibition	Minimum Inhibitory Concentration Assay	Escherichia coli	24 hours	dark conditions
Mn2O3	growth inhibition	Minimum Inhibitory Concentration Assay	Escherichia coli	24 hours	dark conditions
Ni2O3	growth inhibition	Minimum Inhibitory Concentration Assay	Escherichia coli	24 hours	dark conditions
NiO	growth inhibition	Minimum Inhibitory Concentration Assay	Escherichia coli	24 hours	dark conditions
Sb2O3	growth inhibition	Minimum Inhibitory Concentration Assay	Escherichia coli	24 hours	dark conditions

SiO2	growth inhibition	Minimum Inhibitory Concentration Assay	Escherichia coli	24 hours	dark conditions
SnO2	growth inhibition	Minimum Inhibitory Concentration Assay	Escherichia coli	24 hours	dark conditions
TiO2	growth inhibition	Minimum Inhibitory Concentration Assay	Escherichia coli	24 hours	dark conditions
WO3	growth inhibition	Minimum Inhibitory Concentration Assay	Escherichia coli	24 hours	dark conditions
Y2O3	growth inhibition	Minimum Inhibitory Concentration Assay	Escherichia coli	24 hours	dark conditions
Yb2O3	growth inhibition	Minimum Inhibitory Concentration Assay	Escherichia coli	24 hours	dark conditions
ZnO	growth inhibition	Minimum Inhibitory Concentration Assay	Escherichia coli	24 hours	dark conditions
ZrO2	growth inhibition	Minimum Inhibitory Concentration Assay	Escherichia coli	24 hours	dark conditions
Al2O3	viability test	CytoTox-Glo Cytotoxicity Assay	HaCaT cells	24 hours	dark conditions
Bi2O3	viability test	CytoTox-Glo Cytotoxicity Assay	HaCaT cells	24 hours	dark conditions
CoO	viability test	CytoTox-Glo Cytotoxicity Assay	HaCaT cells	24 hours	dark conditions
Cr2O3	viability test	CytoTox-Glo Cytotoxicity Assay	HaCaT cells	24 hours	dark conditions
Fe2O3	viability test	CytoTox-Glo Cytotoxicity Assay	HaCaT cells	24 hours	dark conditions
In2O3	viability test	CytoTox-Glo Cytotoxicity Assay	HaCaT cells	24 hours	dark conditions
La2O3	viability test	CytoTox-Glo Cytotoxicity Assay	HaCaT cells	24 hours	dark conditions
Mn_2O_3	viability test	CytoTox-Glo Cytotoxicity Assay	HaCaT cells	24 hours	dark conditions
NiO	viability test	CytoTox-Glo Cytotoxicity Assay	HaCaT cells	24 hours	dark conditions
Sb2O3	viability test	CytoTox-Glo Cytotoxicity Assay	HaCaT cells	24 hours	dark conditions
SiO2	viability test	CytoTox-Glo Cytotoxicity Assay	HaCaT cells	24 hours	dark conditions
SnO2	viability test	CytoTox-Glo Cytotoxicity Assay	HaCaT cells	24 hours	dark conditions
TiO2	viability test	CytoTox-Glo Cytotoxicity Assay	HaCaT cells	24 hours	dark conditions
V2O3	viability test	CytoTox-Glo Cytotoxicity Assay	HaCaT cells	24 hours	dark conditions
Y2O3	viability test	CytoTox-Glo Cytotoxicity Assay	HaCaT cells	24 hours	dark conditions
ZnO	viability test	CytoTox-Glo Cytotoxicity Assay	HaCaT cells	24 hours	dark conditions
ZrO2	viability test	CytoTox-Glo Cytotoxicity Assay	HaCaT cells	24 hours	dark conditions
WO3	viability test	CytoTox-Glo Cytotoxicity Assay	HaCaT cells	24 hours	dark conditions
Co3O4	growth inhibition	bioluminescence inhibition assay	Photobacterium phosphoreum	12 hours	
Cr2O3	growth inhibition	bioluminescence inhibition assay	Photobacterium phosphoreum	12 hours	
CuO	growth inhibition	bioluminescence inhibition assay	Photobacterium phosphoreum	12 hours	
Fe2O3	growth inhibition	bioluminescence inhibition assay	Photobacterium phosphoreum	12 hours	
Fe3O4	growth inhibition	bioluminescence inhibition assay	Photobacterium phosphoreum	12 hours	
Nd2O3	growth inhibition	bioluminescence inhibition assay	Photobacterium phosphoreum	12 hours	
NiO	growth inhibition	bioluminescence inhibition assay	Photobacterium phosphoreum	12 hours	
Pr6O11	growth inhibition	bioluminescence inhibition assay	Photobacterium phosphoreum	12 hours	
WO3	growth inhibition	bioluminescence inhibition assay	Photobacterium phosphoreum	12 hours	
ZnO	growth inhibition	bioluminescence inhibition assay	Photobacterium phosphoreum	12 hours	
Al2O3	viability test	NRU assay	A549 cells	24 hours	
Co3O4	viability test	NRU assay	A549 cells	24 hours	
CuO	viability test	NRU assay	A549 cells	24 hours	
Fe3O4	viability test	NRU assay	A549 cells	24 hours	
MgO	viability test	NRU assay	A549 cells	24 hours	
Mn3O4	viability test	NRU assay	A549 cells	24 hours	
Sb2O3	viability test	NRU assay	A549 cells	24 hours	
SiO2	viability test	NRU assay	A549 cells	24 hours	
TiO2	viability test	NRU assay	A549 cells	24 hours	
WO3	viability test	NRU assay	A549 cells	24 hours	
ZnO	viability test	NRU assay	A549 cells	24 hours	
Al2O3	viability test	NRU assay	Caco2 cells	24 hours	
Co3O4	viability test	NRU assay	Caco2 cells	24 hours	
CuO	viability test	NRU assay	Caco2 cells	24 hours	
Fe3O4	viability test	NRU assay	Caco2 cells	24 hours	
MgO	viability test	NRU assay	Caco2 cells	24 hours	
Mn3O4	viability test	NRU assay	Caco2 cells	24 hours	
Sb2O3	viability test	NRU assay	Caco2 cells	24 hours	
SiO2	viability test	NRU assay	Caco2 cells	24 hours	
WO3	viability test	NRU assay	Caco2 cells	24 hours	
ZnO	viability test	NRU assay	Caco2 cells	24 hours	
Al2O3	viability test	NRU assay	Balb/c 3T3	24 hours	
Co3O4	viability test	NRU assay	Balb/c 3T3	24 hours	
CuO	viability test	NRU assay	Balb/c 3T3	24 hours	
Fe3O4	viability test	NRU assay	Balb/c 3T3	24 hours	
MgO	viability test	NRU assay	Balb/c 3T3	24 hours	
Mn3O4	viability test	NRU assay	Balb/c 3T3	24 hours	
Sb2O3	viability test	NRU assay	Balb/c 3T3	24 hours	
SiO2	viability test	NRU assay	Balb/c 3T3	24 hours	
WO3	viability test	NRU assay	Balb/c 3T3	24 hours	
ZnO	viability test	NRU assay	Balb/c 3T3	24 hours	
Co3O4	viability test	resazurin fluorescence assay	A549 cells	12 hours	

CuO	viability test	resazurin fluorescence assay	A549 cells	12 hours	
Mn3O4	viability test	resazurin fluorescence assay	A549 cells	12 hours	
Sb2O3	viability test	resazurin fluorescence assay	A549 cells	12 hours	
ZnO	viability test	resazurin fluorescence assay	A549 cells	12 hours	
TiO2	viability test	resazurin fluorescence assay	A549 cells	12 hours	
Co3O4	viability test	resazurin fluorescence assay	Caco2 cells	12 hours	
CuO	viability test	resazurin fluorescence assay	Caco2 cells	12 hours	
Mn3O4	viability test	resazurin fluorescence assay	Caco2 cells	12 hours	
Sb2O3	viability test	resazurin fluorescence assay	Caco2 cells	12 hours	
TiO2	viability test	resazurin fluorescence assay	Caco2 cells	12 hours	
Co3O4	viability test	resazurin fluorescence assay	Balb/c 3T3	12 hours	
CuO	viability test	resazurin fluorescence assay	Balb/c 3T3	12 hours	
Mn3O4	viability test	resazurin fluorescence assay	Balb/c 3T3	12 hours	
Sb2O3	viability test	resazurin fluorescence assay	Balb/c 3T3	12 hours	
ZnO	viability test	resazurin fluorescence assay	Balb/c 3T3	12 hours	
TiO2	viability test	resazurin fluorescence assay	Balb/c 3T3	12 hours	
Al2O3	growth inhibition	bioluminescence inhibition assay	Vibrio fischeri	30 minutes	
Co3O4	growth inhibition	bioluminescence inhibition assay	Vibrio fischeri	30 minutes	
CuO	growth inhibition	bioluminescence inhibition assay	Vibrio fischeri	30 minutes	
Fe3O4	growth inhibition	bioluminescence inhibition assay	Vibrio fischeri	30 minutes	
MgO	growth inhibition	bioluminescence inhibition assay	Vibrio fischeri	30 minutes	
Mn3O4	growth inhibition	bioluminescence inhibition assay	Vibrio fischeri	30 minutes	
Sb2O3	growth inhibition	bioluminescence inhibition assay	Vibrio fischeri	30 minutes	
SiO2	growth inhibition	bioluminescence inhibition assay	Vibrio fischeri	30 minutes	
TiO2	growth inhibition	bioluminescence inhibition assay	Vibrio fischeri	30 minutes	
WO3	growth inhibition	bioluminescence inhibition assay	Vibrio fischeri	30 minutes	
ZnO	growth inhibition	bioluminescence inhibition assay	Vibrio fischeri	30 minutes	
Al2O3	growth inhibition	growth inhibition assay	Pseudokirchneriella subcapitata	72 hours	dark conditions
Co3O4	growth inhibition	growth inhibition assay	Pseudokirchneriella subcapitata	72 hours	dark conditions
CuO	growth inhibition	growth inhibition assay	Pseudokirchneriella subcapitata	72 hours	dark conditions
Fe3O4	growth inhibition	growth inhibition assay	Pseudokirchneriella subcapitata	72 hours	dark conditions
MgO	growth inhibition	growth inhibition assay	Pseudokirchneriella subcapitata	72 hours	dark conditions
Mn3O4	growth inhibition	growth inhibition assay	Pseudokirchneriella subcapitata	72 hours	dark conditions
Sb2O3	growth inhibition	growth inhibition assay	Pseudokirchneriella subcapitata	72 hours	dark conditions
SiO2	growth inhibition	growth inhibition assay	Pseudokirchneriella subcapitata	72 hours	dark conditions
TiO2	growth inhibition	growth inhibition assay	Pseudokirchneriella subcapitata	72 hours	dark conditions
WO3	growth inhibition	growth inhibition assay	Pseudokirchneriella subcapitata	72 hours	dark conditions
ZnO	growth inhibition	growth inhibition assay	Pseudokirchneriella subcapitata	72 hours	dark conditions
Al2O3	viability test	ATP assay	Tetrahymena thermophile	24 hours	dark conditions
Co3O4	viability test	ATP assay	Tetrahymena thermophile	24 hours	dark conditions
CuO	viability test	ATP assay	Tetrahymena thermophile	24 hours	dark conditions
Fe3O4	viability test	ATP assay	Tetrahymena thermophile	24 hours	dark conditions
MgO	viability test	ATP assay	Tetrahymena thermophile	24 hours	dark conditions
Mn3O4	viability test	ATP assay	Tetrahymena thermophile	24 hours	dark conditions
Sb2O3	viability test	ATP assay	Tetrahymena thermophile	24 hours	dark conditions
SiO2	viability test	ATP assay	Tetrahymena thermophile	24 hours	dark conditions
TiO2	viability test	ATP assay	Tetrahymena thermophile	24 hours	dark conditions
WO3	viability test	ATP assay	Tetrahymena thermophile	24 hours	dark conditions
ZnO	viability test	ATP assay	Tetrahymena thermophile	24 hours	dark conditions